Two-Dimensional NMR Studies of Staphylococcal Nuclease: Evidence for Conformational Heterogeneity from Hydrogen-1, Carbon-13, and Nitrogen-15 Spin System Assignments of the Aromatic Amino Acids in the Nuclease H124L-Thymidine 3',5'-Bisphosphate-Ca^{2+} Ternary Complex†

Jinfeng Wang, Andrew P. Hinck,‡ Stewart N. Loh,§ and John L. Markley*

Department of Biochemistry, College of Agricultural and Life Sciences, University of Wisconsin—Madison, 420 Henry Mall, Madison, Wisconsin 53706

Received November 15, 1989; Revised Manuscript Received January 9, 1990

ABSTRACT: A combination of multinuclear two-dimensional NMR experiments served to identify and assign the combined ^1H, ^{13}C, and ^{15}N spin systems of the single tryptophan, three phenylalanines, three histidines, and seven tyrosines of staphylococcal nuclease H124L in its ternary complex with calcium and thymidine 3',5'-bisphosphate at pH 5.1 (H_2O) or pH* 5.5 (^2H_2O). Samples of recombinant nuclease were labeled with ^{13}C or ^{15}N as appropriate to individual NMR experiments: uniformly with ^{15}N (all sites to >95%), uniformly with ^{13}C (all sites to 26%), selectively with ^{13}C (single amino acids uniformly labeled to 26%), or selectively with ^{15}N (single amino acids uniformly labeled to >95%). NMR data used in the analysis included single-bond and multiple-bond ^1H–^{13}C and multiple-bond ^1H–^{15}N correlations, ^1H–^{13}C single-bond correlation with Hartmann–Hahn relay ($^1H\{^{13}C\}$SBC-HH), and ^1H–^{13}C single-bond correlation with NOE relay ($^1H\{^{13}C\}$SBC-NOE). The aromatic protons of the spin systems were identified from $^1H\{^{13}C\}$SBC-HH data, and the nonprotonated aromatic ring carbons were identified from ^1H–^{13}C multiple-bond correlations. Sequence-specific assignments were made on the basis of observed NOE relay connectivities between assigned $^1H^{\alpha}$–$^{13}C^{\alpha}$ or $^1H^{\beta}$–$^{13}C^{\beta}$ direct cross peaks in the aliphatic region [Wang, J., LeMaster, D. M., & Markley, J. L. (1990) *Biochemistry 29*, 88–101] and $^1H^{\delta}$–$^{13}C^{\delta}$ direct cross peaks in the aromatic region of the $^1H\{^{13}C\}$SBC-NOE spectrum. The His^{121} $^1H^{\delta_2}$ resonance, which has an unusual upfield shift (at 4.3 ppm in the aliphatic region), was assigned from $^1H\{^{13}C\}$SBC, $^1H\{^{13}C\}$MBC, and $^1H\{^{15}N\}$MBC data. Evidence for local structural heterogeneity in the ternary complex was provided by doubled peaks assigned to His^{46}, one tyrosine, and one phenylalanine. Measurement of NOE buildup rates between protons on different aromatic residues of the major ternary complex species yielded a number of interproton distances that could be compared with those from X-ray structures of the wild-type nuclease ternary complex with calcium and thymidine 3',5'-bisphosphate [Cotton, F. A., Hazen, E. E., Jr., & Legg, M. J. (1979) *Proc. Natl. Acad. Sci. U.S.A. 76*, 2551–2555; Loll, P. J., & Lattman, E. E. (1989) *Proteins: Struct., Funct., Genet. 5*, 183–201]. The unusual chemical shift of His^{121} $^1H^{\delta_2}$ is consistent with ring current calculations from either X-ray structure.

The V8 variant of *Staphylococcus aureus* produces a nuclease (nuclease H124L)[1] that contains 14 aromatic amino acid residues: one tryptophan, three phenylalanines, seven tyrosines, and three histidines (Taniuchi et al., 1967). The aromatic residues of this nuclease and that from the Foggi variant (nuclease wt),[2] which differs from the V8 variant by substitution of histidine for leucine at position 124 (Cusumano et al., 1968), have been the object of NMR investigation since the mid 1960s. Signals from the tyrosines and tryptophan were identified initially by selective deuteration of the aromatic amino acid residues (Markley et al., 1968). Signals from tyrosines 85, 113, and 115 were assigned tentatively on the basis of selective nitration experiments (Cohen et al., 1971). Recent developments in two-dimensional NMR methodology have permitted extensive sequence-specific NMR assignments in staphylococcal nucleases (Torchia et al., 1989a; Wang et al., 1990a,b).

^1H NMR signals from the $^1H^{\epsilon_1}$ atoms of the His rings were observed first at 100 MHz (Meadows et al., 1967). The initial assignments of the His $^1H^{\epsilon_1}$ signals (Jardetzky et al., 1972) were confirmed by mutagenesis studies (Alexandrescu et al., 1988). Interest in the histidines has revived recently. Doubling of the His ^1H NMR signals (Markley et al., 1970) provides a means of studying equilibria that link multiple conformational substates of the enzyme (Fox et al., 1986; Evans et al., 1987, 1989; Alexandrescu et al., 1988, 1989; Alexandrescu, 1989). Separate His resonances are found for two monomeric forms and a dimeric form of the enzyme. The structural heterogeneity that gives rise to the two monomer peaks has been attributed to cis/trans isomerism of the Lys^{116}–Pro^{117} peptide bond (Evans et al., 1987). This heterogeneity is decreased upon formation of the nuclease·Ca^{2+}·pdTp ternary complex. X-ray structures of the ternary complex show the Lys^{116}–Pro^{117} peptide bond to be cis (Cotton et al., 1979; Loll & Lattman, 1989), and this result has been confirmed for the

†Supported by Grant GM35976 from the National Institutes of Health and by a NEDO grant from the Japanese Government. This study made use of the National Magnetic Resonance Facility at Madison, which is supported in part by NIH Grant RR02301 from the Biomedical Research Technology Program, Division of Research Resources. Equipment in the facility was purchased with funds from the University of Wisconsin, the NSF Biological Biomedical Research Technology Program (DMB-8415048), the NIH Biomedical Research Technology Program (RR02301), the NIH Shared Instrumentation Program (RR02781), and the U.S. Department of Agriculture.

‡Trainee supported by a Training Grant in Biophysics (NIH GM08293).

§Trainee supported by a Training Grant in Cellular and Molecular Biology (NIH GM07215).

0006-2960/90/0429-4242$02.50/0

ternary complex in solution (Torchia et al., 1989b). Stanczyk et al. (1988) have reported that the His^{121} $^1H^{\delta_2}$ resonance of nuclease wt is split as the consequence of local conformational heterogeneity that is not removed upon formation of the ternary complex.

This paper, which is the third in a series (Wang et al., 1990a,b) on the ^1H, ^{13}C, and ^{15}N NMR assignments and solution structure of staphylococcal nuclease H124L, presents complete assignments of the aromatic ^1H, ^{13}C, and ^{15}N spin systems of the nuclease H124L·Ca^{2+}·pdTp ternary complex at pH 5.1 (for soltuions in H_2O) or pH* 5.5 (for solutions in ^2H_2O).[3] In making these assignments, we employed, in addition to nuclease H124L samples used previously that were at natural abundance or labeled uniformly with ^{13}C and ^{15}N (Wang et al., 1990b), nuclease H124L samples that were labeled selectively with [26% U-^{13}C]-L-Tyr, [26% U-^{13}C]-L-Phe, [26% U-^{13}C]-L-His, or [95% U-^{15}N]-L-His. In the course of this work, we found an unusual chemical shift for the His^{121} $^1H^{\delta_2}$ (slightly upfield of the water resonance at 4.3 ppm in the aliphatic region). The chemical shift of this proton had been reported earlier at 6.3 ppm (Stanczyk et al., 1988). Both the crystal (Cotton et al., 1979; Loll & Lattman, 1989) and solution structural results place the His^{121} $^1H^{\delta_2}$ adjacent to the middle of the aromatic ring of Tyr^{91}. The chemical shift of 4.3 ppm is in agreement with ring-current calculations from X-ray coordinates (Cotton et al., 1979; Loll & Lattman, 1989). We have discovered the presence of conformational heterogeneity within the ternary complex as reported by doubling of ^1H, ^{13}C, and ^{15}N resonances assigned to His^{46}.

Experimental Procedures

Protein Samples. Nine solutions of the ternary complex were studied, each of which provided a different pattern of stable isotope labeling: (1) [na]H124L-TC in 100% ^2H_2O containing 3.5 mM protein, 10.5 mM dpTp, 21 mM $CaCl_2$, and 0.3 M KCl at pH* 5.5; (2) [95% U-^{15}N]H124L-TC in 100% ^2H_2O containing 5 mM protein, 15 mM pdTp, 30 mM $CaCl_2$, and 0.3 M KCl at pH* 5.5; (3) [95% U-^{15}N]H124L-TC in 90% H_2O/10% ^2H_2O containing 5 mM protein, 15 mM pdTp, 30 mM $CaCl_2$, and 0.3 M KCl at pH 5.1; (4) [95% U-^{15}N]His-H124L-TC in 100% ^2H_2O containing 5 mM protein, 15 mM pdTp, 30 mM $CaCl_2$, and 0.3 M KCl at pH* 5.5; (5) [95% U-^{15}N]His-H124L-TC in 90% H_2O/10% ^2H_2O containing 5 mM protein, 15 mM pdTp, 30 mM $CaCl_2$, and 0.3 M KCl at pH 5.1; (6) [26% U-^{13}C]H124L-TC in 100% ^2H_2O containing 5 mM protein, 15 mM pdTp, 30 mM $CaCl_2$, and 0.3 M KCl at pH* 5.5; (7) [26% U-^{13}C]Tyr-H124L-TC in 100% ^2H_2O containing 5 mM protein, 15 mM pdTp, 30 mM $CaCl_2$, and 0.3 M KCl at pH* 5.5; (8) [26% U-^{13}C]Phe-H124L-TC in 100% ^2H_2O containing 5 mM protein, 15 mM pdTp, 30 mM $CaCl_2$, and 0.3 M KCl at pH* 5.5; (9) [26% U-^{13}C]His-H124L-TC in 100% ^2H_2O containing 5 mM protein, 15 mM pdTp, 30 mM $CaCl_2$, and 0.3 M KCl at pH* 5.5.

Methods described previously were used to prepare nuclease samples labeled with ^{13}C and ^{15}N (Wang et al., 1990b), to isolate and purify the protein samples (Alexandrescu et al., 1988), and to prepare the ternary complexes (Wang et al., 1990a). Uniformly ^{13}C-labeled amino acids were prepared as described by Grissom and Markley (1989). The sample of [95% U-^{15}N]His used to make the selectively labeled nuclease was a generous gift from M. Kainosho (Tokyo Metropolitan University).

NMR Spectroscopy. Homonuclear and heteronuclear two-dimensional $^1H\{^1H\}$, $^1H\{^{13}C\}$, and $^1H\{^{15}N\}$ NMR data were collected on a Bruker AM 500 or AM 600 spectrometer at a temperature setting of 45 °C. As in the previous studies (Wang et al., 1990a,b), ^1H, ^{13}C, and ^{15}N chemical shifts are quoted relative to those of internal TSP, external 10% dioxane in ^2H_2O (at an assumed chemical shift of 67.8 ppm relative to that of TMS), or 95% $(^{15}NH_4)_2SO_4$ in 90% H_2O/10% ^2H_2O (at an assumed chemical shift of 21.6 ppm relative to that of liquid ammonia), respectively.

Two-dimensional $^1H\{^1H\}$ phase-sensitive DQF-COSY, HOHAHA, and NOESY spectra were acquired with [na]-H124L-TC samples. ^{13}C- or ^{15}N-labeled H124L-TC samples were used in acquiring 2D ^1H-detected heteronuclear correlated spectra. The $^1H\{^{13}C\}$ data sets were collected for the aromatic region alone, but the $^1H\{^{13}C\}$SBC-NOE data covered both the aromatic and aliphatic regions. The $^1H\{^{15}N\}$ data were acquired for the His region only. The NMR methodology and experimental parameters were as described in detail in the previous papers (Wang et al., 1990a,b). The figure legends describe essential features pertaining to the 2D NMR spectra shown.

Interproton Distance Calculations. NOESY data for the nuclease ternary complex were obtained at three mixing times (τ_c = 100, 150, and 200 ms). Intensities of cross peaks in the aromatic region were measured, and interproton distances were calculated from the NOE buildup rates as described by Fejzo et al. (1989). In making these calculations, a uniform correlation time was assumed to hold for all NOEs. A correlation time of 7 ns was determined experimentally by fitting the NOE buildup rates betwen pairs of protons separated by known distances: the intraresidue NOEs between $^1H^{\delta}$ and $^1H^{\zeta}$ of Phe^{76} (distance = 4.3 Å) and the intraresidue NOEs between

[1] Abbreviations: 2D, two dimensional; DQF-COSY, two-dimensional double quantum filtered phase-sensitive homonuclear correlated spectroscopy; HOHAHA, two-dimensional Hartmann–Hahn magnetization transfer spectroscopy; NOE, nuclear Overhauser enhancement; NOESY, two-dimensional dipolar correlated spectroscopy; NM, native (folded form of nuclease); U, unfolded form of nuclease; BC, nuclease·Ca^{2+} binary complex; TC, nuclease·pdTp·Ca^{2+} ternary complex; a1, subconformation of nuclease whose relative abundance increases upon pdTp·Ca^{2+} binding; a2, subconformation of nuclease whose relative abundance decreases upon pdTp·Ca^{2+} binding; b1 and b2, subconformations of nuclease identified by doubling of the His^{46} $^1H^{\epsilon_1}$ resonance (in nuclease H124L at pH 5.5 and 318 K, b1 is defined as the form giving rise to the higher intensity and higher field His^{46} $^1H^{\epsilon_1}$ signal, and b2 is defined as the form giving rise to the smaller intensity and lower field His^{46} $^1H^{\epsilon_1}$ signal); $Phe^?$ ($F^?$) and $Tyr^?$ ($Y^?$), unassigned extra spin systems from phenylalanine and tyrosine, respectively; His_U or U, signal from histidine in unfolded (denanatured or degraded) protein; nuclease H124L, mutant of the nuclease from *Staphylococcus aureus* (Foggi strain) (EC 3.14.7) in which the histidine at residue 124 has been replaced with leucine; [na]H124L-TC, ternary complex prepared with natural abundance (unlabeled) nuclease H124L; [26% U-^{13}C]H124L-TC, ternary complex made with nuclease enriched uniformly with ^{13}C to 26% isotope; [95% U-^{15}N]H124L-TC, ternary complex made with nuclease enriched uniformly with ^{15}N to >95% isotope; [26% U-^{13}C]Phe-H124L-TC, ternary complex made with nuclease that contains phenylalanine enriched uniformly with ^{13}C to 26% isotope; [26% U-^{13}C]Tyr-H124L-TC, ternary complex made with nuclease that contains tyrosine enriched uniformly with ^{13}C to 26% isotope; [26% U-^{13}C]His-H124L-TC, ternary complex made with nuclease that contains histidine enriched uniformly with ^{13}C to 26% isotope; [95% U-^{15}N]His-H124L-TC, ternary complex made with nuclease that contains histidine enriched uniformly with ^{15}N to >95% isotope; pdTp, thymidine 3′,5′-bisphosphate; TSP, 3-(trimethylsilyl)[$^2H_4$]propionate; pH*, uncorrected pH meter reading of a ^2H_2O solution with a glass electrode standardized with H_2O buffers. Cross-peak positions in spectra are given as *X*,*Y* ppm, where *X* is the horizontal axis and *Y* is the vertical axis.

[2] By general usage, the nuclease from the Foggi strain of *Staphylococcus aureus* is defined at the wild-type enzyme. Nuclease H124L technically is the wild-type nuclease from the V8 strain of *Staphylococcus aureus*.

[3] The exact number of calcium ions bound in the ternary complex (one or two) is controversial (Tucker et al., 1979).

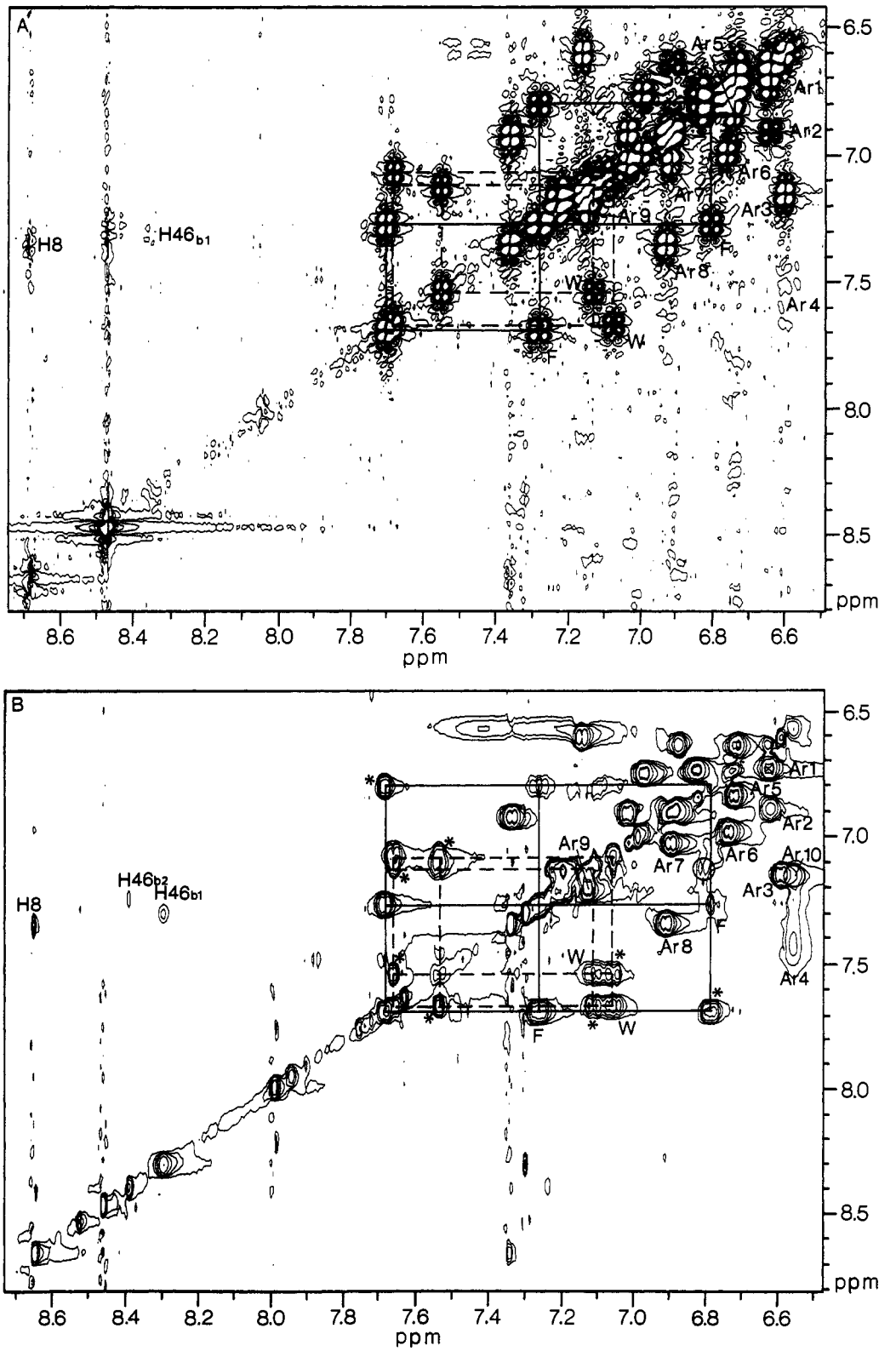

FIGURE 1: Two-dimensional $^1H\{^1H\}$ correlated NMR spectra (500 MHz) of nuclease H124L TC in ^2H_2O solution, pH* 5.5. (A) Aromatic region of the phase-sensitive DQF-COSY spectrum collected over a 6500-Hz spectral width with 512 increments and 128 averaged FIDs for each t_1 value. Shifted sine bell window functions were used in both dimensions for resolution enhancement. Double zero-filling was used to extend the t_1 dimension to 2048 points prior to Fourier transformation. Both positive and negative contour levels are shown in this presentation. (B) Aromatic region of the HOHAHA spectrum collected as 512 increments with a mixing time of 55 ms and with 136 averaged FIDs per t_1 value. Other spectral parameters were as given above for the COSY experiment. Relayed cross peaks are denoted by asterisks. The spin system of the Trp residue is indicated by dashed lines and those of Phe residues are indicated by continuous lines. Cross peaks from His are labeled by the one-letter amino acid code and residue number; other cross peaks are labeled with "Ar" followed by an arbitrary number.

$^1H^\delta$ and $^1H^\epsilon$ of Tyr^{27}, Tyr^{85}, and Tyr^{113} (distance = 2.5 Å). Experimental distances were determined by measuring cross-peak intensities as a function of mixing time, normalizing these against the intensities of corresponding diagonal peaks, and using the results to generate the NOE buildup curve. An initial rate approximation was used to calculate the distances.

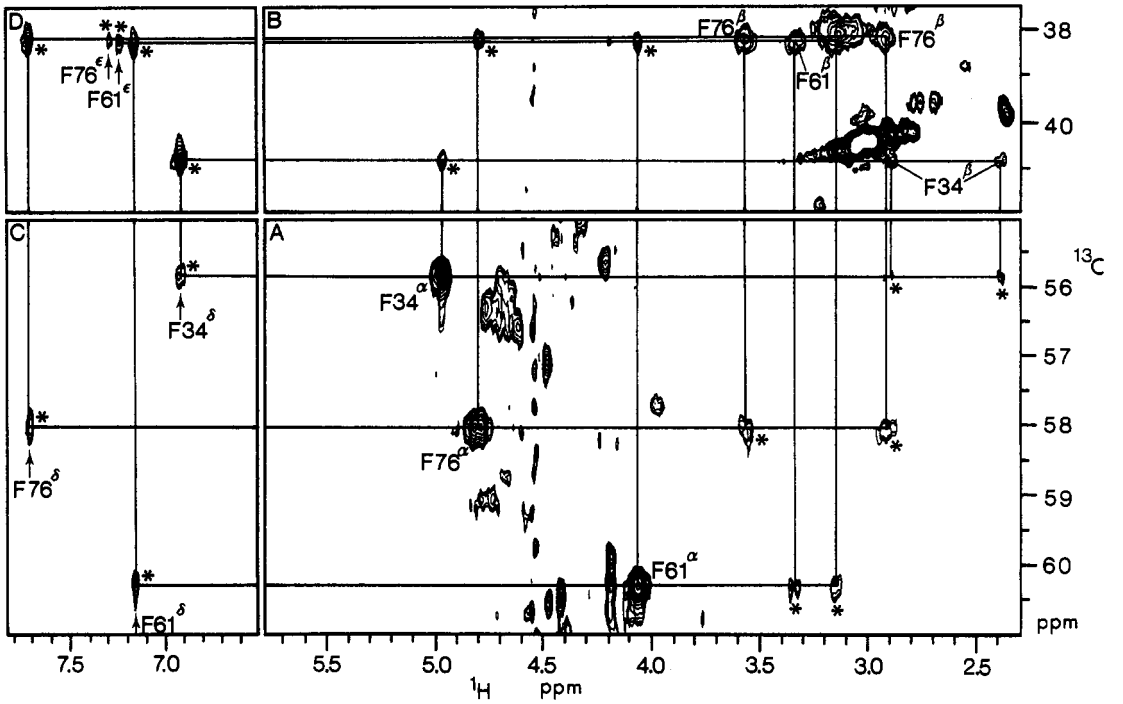

FIGURE 2: Four parts of the two-dimensional $^1H\{^{13}C\}$SBC-NOE spectrum (500 MHz) of [26% U-^{13}C]Phe-H124L-TC in ^2H_2O, pH* 5.5. The spectral range covered only the aliphatic region. 340 increments were collected with 304 averaged FIDs per t_1 value. The mixing time used for the NOE buildup was 250 ms. Shifted sine bell filtering was used in t_1, and a Gaussian function was used in t_2. Zero-filling to 2048 points was applied in the t_1 dimension. The NOE relay cross peaks are indicated by asterisks. Single-bond correlation cross peaks are labeled by the one-letter amino acid code and residue number. (A) Region containing Phe $^1H^{\alpha}$–$^{13}C^{\alpha}$ direct cross peaks and $^1H^{\beta,\beta'}$–$^{13}C^{\alpha}$ NOE relay cross peaks. (B) Region containing Phe $^1H^{\beta,\beta'}$–$^{13}C^{\beta}$ direct cross peaks and $^1H^{\alpha}$–$^{13}C^{\beta}$ NOE relay cross peaks. (C) Region containing Phe $^1H^{\delta}$–$^{13}C^{\alpha}$ NOE relay cross peaks. (D) Region containing Phe $^1H^{\delta,\epsilon}$–$^{13}C^{\beta}$ NOE relay cross peaks.

The standard deviation of the fit was on the order of 10–20%.

Ring-Current Calculations. Ring-current calculations according to the current-loop model of Johnson and Bovey (1958) were carried out by use of the FORTRAN program RCUR4 adapted from Perkins (1982) to run on a Silicon Graphics Iris 4D/220GTX workstation (A. M. Krezel and C. L. Kojiro, unpublished data). Input data for the ring-current calculations were derived by adding hydrogens to the heavy atom coordinates obtained from the Protein Data Bank with the MOLEDIT routine of the INSIGHT software package (Biosym Technologies, Inc.). The FORTRAN program DIST2 (A. M. Krezel, unpublished data) was used to extract interproton distances from the structure.

RESULTS

Assignment Strategy. Aromatic amino acid residue assignments are based, most commonly, on the separate identification of the aromatic and aliphatic components of each spin system followed by their linkage on the basis of intraresidue NOEs between aromatic $^1H^{\delta}$ and aliphatic $^1H^{\alpha}$ and $^1H^{\beta,\beta'}$ protons. According to the amino acid composition of nuclease H124L, one expects to find a maximum of 19 cross peaks in the aromatic region of the COSY map. Twelve strong and several weak cross peaks were observed in the DQF-COSY spectrum collected in ^2H_2O (Figure 1A). The spin systems of the single tryptophan and one phenylalanine were identified readily by comparison of DQF-COSY and HOHAHA (^2H_2O) data (Figure 1, solid and dashed lines, respectively, for Phe and Trp). However, spectral ambiguities interfered with further spin system identifications. In order to obtain rigorous assignments, it was necessary to make use of uniform and selective ^{13}C and ^{15}N labeling in conjunction with multinuclear 2D NMR spectroscopy. The present assignments relied heavily on ^{1}H-detected, ^{13}C- or ^{15}N-correlated, 2D NMR experiments (Markley, 1989).

The sequence-specific backbone assignments established in the previous papers (Wang et al., 1990a,b) included those from all aromatic residues. The $^1H^{\alpha}$ assignments of the aromatic residues provided starting points for the full assignments of their spin systems. $^1H\{^{13}C\}$SBC and $^1H\{^{13}C\}$SBC-HH data were used to elucidate the aromatic and aliphatic portions of the proton and carbon spin systems. $^1H\{^{13}C\}$SBC-HH spectroscopy of the aromatic region was of particular importance in identifying the ring proton spin systems of each aromatic residue. The $^1H\{^{13}C\}$SBC-HH experiment as tailored for the aromatic region provided a reliable approach for distinguishing Tyr and Phe spin systems. Intraresidue NOEs between $^1H^{\alpha,\beta}$ and $^1H^{\delta,\epsilon}$ provided the links between the aliphatic and aromatic portions of the spin systems of each amino acid. $^1H\{^{13}C\}$-SBC-NOE spectroscopy proved essential for site-specific assignments of aromatic ring proton and carbon resonances. Multiple-bond ^1H–^{13}C correlations were used to assign quaternary carbon resonances. Single-bond and multiple-bond ^1H–^{15}N correlations were used to assign nitrogen resonances. All of the assignments are summarized in Table I.

Assignment of the Aliphatic AMX Proton Spin Systems and Their Associated Carbon Spin Systems. The $^1H^{\alpha}$–$^{13}C^{\alpha}$ direct cross peaks of Tyr and Phe, respectively, were identified in $^1H\{^{13}C\}$SBC spectra of [26% U-^{13}C]Tyr-H124L-TC or [26% U-^{13}C]Phe-H124L-TC. Further comparison of these spectra with $^1H\{^{13}C\}$SBC-NOE spectra of the same selectively labeled complexes allowed us to assign $^1H^{\beta}$–$^{13}C^{\beta}$ direct cross peaks for each aromatic residue. Figure 2 shows the $^1H\{^{13}C\}$SBC-NOE spectrum of [26% U-^{13}C]Phe-H124L-TC. The pairs of $^1H^{\beta,\beta'}$–$^{13}C^{\alpha}$ NOE relay cross peaks in the region 2.30–3.70,55.5–60.5 ppm (Figure 2A) and the three $^1H^{\alpha}$–$^{13}C^{\beta}$ NOE relay cross peaks in the region 4.0–5.10,38.0–41.0 ppm (Figure 2B) established connectivities between the $^1H^{\alpha}$–$^{13}C^{\alpha}$ and $^1H^{\beta}$–$^{13}C^{\beta}$ direct cross peaks.

By selective labeling of the tyrosines so as to eliminate

Table I: Resonance Assignments for the Aromatic Amino Acid Residues of the Staphylococcal Nuclease H124L Ternary Complex at 45 °C[a]

	Tyr^{27}	Tyr^{54}	Tyr^{85}	Tyr^{91}	$Tyr^{?}$	Tyr^{93}	Tyr^{113}	Tyr^{115}	Phe^{34}	Phe^{61}	$Phe^{?}$	Phe^{76}	His^{8}	His_{U}	$His^{46}{}_{b2}$	$His^{46}{}_{b1}$	His^{121}	Trp^{140}
$^1H^{\alpha}$	5.06	4.39	4.65	4.63		5.11	3.44	5.03	4.94	4.05		4.77	5.04			4.89	5.47	4.91
$^1H^{\beta}$	3.01	3.18	2.88	3.40		2.37	2.57	3.00	2.37	3.14		2.92	3.26			3.12	2.35	2.83
$^1H^{\beta'}$	3.19		3.39			2.84	2.97	3.11	2.89	3.33		3.55	3.33			3.17	3.28	3.71
$^1H^{\delta_1}$	7.34	6.82	7.02	7.15/ 7.46[b]	7.13	6.63	6.98	7.15	6.89	7.13	7.23	7.69						7.00
$^1H^{\delta_2}$	7.34	6.82	7.02	7.15/ 7.46[b]	7.13	6.63	6.98	7.15	6.89	7.13	7.23	7.69	7.35	7.30	7.26	7.31	4.32	
$^1H^{\epsilon_1}$	6.92	6.73	6.91	6.58	6.81	6.73	6.74	6.60	6.91	7.21	7.34	7.27	8.66	8.53	8.40	8.31	8.01	
$^1H^{\epsilon_2}$	6.92	6.73	6.91	6.58	6.81	6.73	6.74	6.60	6.91	7.21	7.34	7.27						
$^1H^{\epsilon_3}$																		7.66
$^1H^{\zeta}$									6.64	7.19	7.28	6.79						
$^1H^{\zeta_2}$																		7.54
$^1H^{\zeta_3}$																		7.06
$^1H^{\eta}$																		7.12
$^{13}C^{\alpha}$	55.2	54.7	55.9	56.2		54.7	55.9	53.3	55.8	60.3		58.0	53.4			52.8	51.9	53.5
$^{13}C^{\beta}$	40.2	37.1	36.7	36.2		36.2		36.8	40.8	38.3		38.2	29.5			29.0	27.2	28.5
$^{13}C^{\gamma}$	127.4	128.7	129.9		129.3	130.5	130.3	129.4	138.6	136.2	137.3	138.4	129.7		130.4	132.1	130.8	109.7
$^{13}C^{\delta_1}$	132.2	130.9	131.1		131.7	131.0	131.1	132.1	129.7	130.8	130.4	131.2						126.4
$^{13}C^{\delta_2}$	132.2	130.9	131.1		131.7	131.0	131.1	132.1	129.7	130.8	130.4	131.2	118.7		118.5	118.6	117.8	127.2
$^{13}C^{\epsilon_1}$	116.7	116.8	116.9	116.6/ 118.1[b]	116.6	116.4	116.3	115.8	129.7	129.1	129.9	129.6	135.1	135.1	135.5	136.1	136.4	
$^{13}C^{\epsilon_2}$	116.7	116.8	116.9	116.6/ 118.1[b]	116.6	116.4	116.3	115.8	129.7	129.1	129.9	129.6						138.4
$^{13}C^{\epsilon_3}$																		119.6
$^{13}C^{\zeta}$	156.7	155.7	156.2		155.6	156.5	155.9	155.3	128.2	128.3	128.4	127.3						
$^{13}C^{\zeta_2}$																		113.2
$^{13}C^{\zeta_3}$																		119.6
$^{13}C^{\eta}$																		122.4
$^{15}N^{\delta_1}$													179.60	182.78	193.47		213.39	
$^{15}N^{\delta_2}$													174.40	174.69	174.69	171.8	170.07	

[a] ^{13}C and ^{15}N data were collected at pH* 5.5 in ^2H_2O solution. The $^{13}C^{\alpha}$ and $^{13}C^{\beta}$ chemical shift values were taken from $^1H\{^{13}C\}$SBC-NOE data; chemical shifts of most protons were taken from $^1H\{^1H\}$ 2D NMR data. ^{15}N chemical shifts were taken from $^1H\{^{15}N\}$MBC data. [b] The Tyr^{91} ring, which flips slowly on the NMR time scale, has separate signals for atoms on either side of the ring.

Table II: Distances between Pairs of Aromatic Ring Hydrogens That Show Interresidue NOE Connectivities in Two-Dimensional NOESY Spectra of the Nuclease H124L Ternary Complex at pH* 5.5

hydrogen pairs[a]				distances (Å)			hydrogen pairs[a]				distances (Å)		
				X-ray crystal		NMR solution					X-ray crystal		NMR solution
residue	atom	residue	atom	Cotton et al. (1979)	Loll and Lattman (1989)	present work[b]	residue	atom	residue	atom	Cotton et al. (1979)	Loll and Lattman (1989)	present work[b]
Tyr^{113}	δ_2	Tyr^{115}	ϵ_1	5.3	3.5	3.9	Phe^{76}	δ_1	Tyr^{27}	ϵ_1	4.3	5.0	<5
	δ_2		ϵ_2	2.3	4.3		Phe^{76}	ζ	Phe^{34}	ϵ_2	7.1	2.7	2.7[c]
	δ_1		ϵ_1	8.7	6.0			ζ		δ_2	9.3	3.9	
	δ_1		ϵ_2	4.5	8.2		Phe^{76}	ϵ_1	Phe^{34}	ζ	5.9	4.2	<5
Phe^{34}	ζ	Tyr^{27}	δ_1	4.6	4.3	4.0		ϵ_2		ζ	8.1	4.2	
	ζ		δ_2	2.1	3.4		Phe^{76}	ϵ_1	Phe^{34}	ϵ_2	5.9	4.3	3.6[c]
Phe^{76}	ϵ_1	Tyr^{27}	ϵ_1	4.0	3.5	3.4		ϵ_2		ϵ_2	7.3	2.7	
	ϵ_1		ϵ_2	2.1	3.4			ϵ_2		δ_2	9.0	4.2	

[a] Because of rapid ring flips, the chemical shifts of the δ_1 and δ_2 ring protons and ϵ_1 and ϵ_2 rings protons are averaged. Thus, one cannot distinguish one side of the ring from the other by NMR. [b] The NMR distances are probably accurate to within ±1 Å. [c] The chemical shifts of Phe^{34} $^1H^{\delta_1,\delta_2}$ and $^1H^{\epsilon_1,\epsilon_2}$ are very similar.

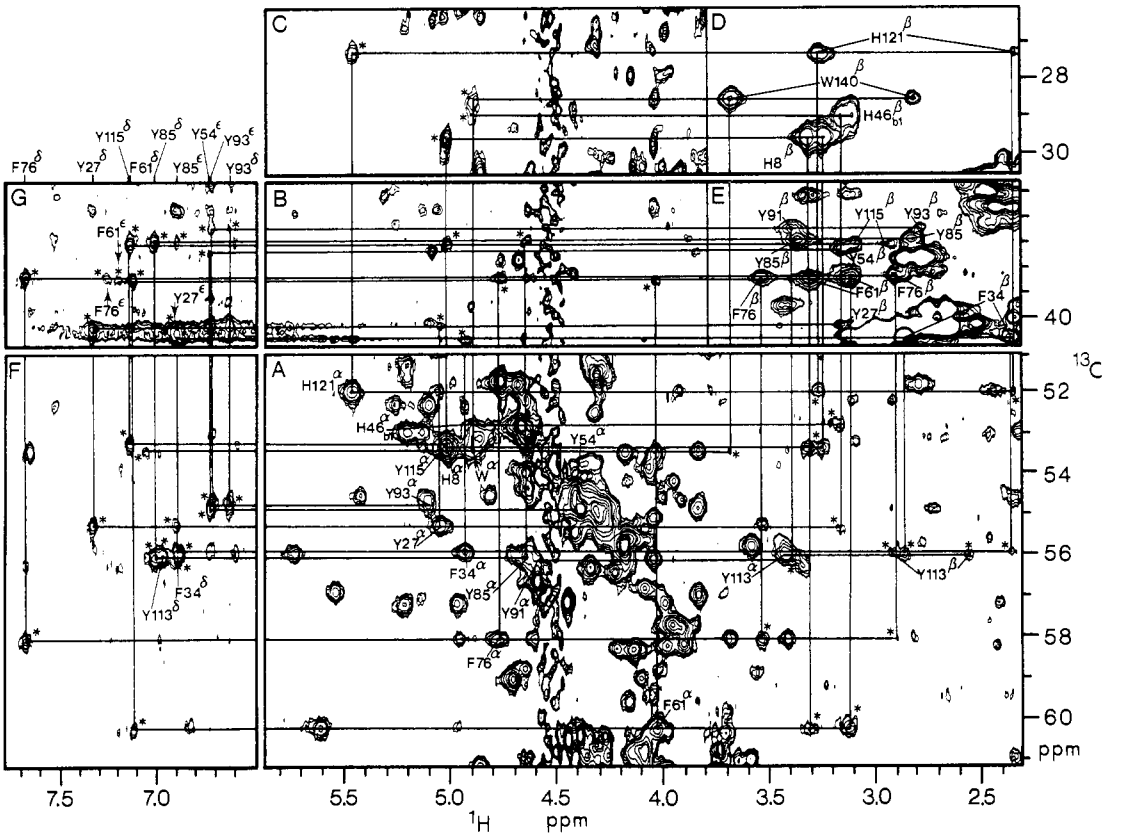

FIGURE 3: Combined presentation of $^1H\{^{13}C\}$SBC (600 MHz) and $^1H\{^{13}C\}$SBC-NOE (500 MHz) spectra of [26% U-^{13}C]H124L-TC in ^2H_2O. The $^1H\{^{13}C\}$SBC spectrum consisted of 512 blocks recorded with 96 averaged FIDs per t_1 value. The $^1H\{^{13}C\}$SBC-NOE spectrum consisted of 460- blocks recorded with 160 averaged FIDs per t_1 value; the mixing time for NOE buildup was 250 ms. Additional spectral parameters and data processing procedures were as described above (Figure 2). Single-bond correlation cross peaks are labeled by the one-letter amino acid code and residue number; NOE relay cross peaks are indicated by asterisks. (A) Region containing $^1H^{\alpha}$–$^{13}C^{\alpha}$ direct cross peaks and $^1H^{\beta}$–$^{13}C^{\alpha}$ NOE relay cross peaks of aromatic amino acid residues. (B and C) Region containing $^1H^{\alpha}$–$^{13}C^{\beta}$ NOE relay cross peaks. (D and E) Region containing $^1H^{\beta}$–$^{13}C^{\beta}$ direct cross peaks of $^1H\{^{13}C\}$SBC spectrum. (F) Region containing $^1H^{\delta,\epsilon}$–$^{13}C^{\alpha}$ NOE relay cross peaks. (G) Region containing $^1H^{\delta}$–$^{13}C^{\beta}$ NOE relay cross peaks.

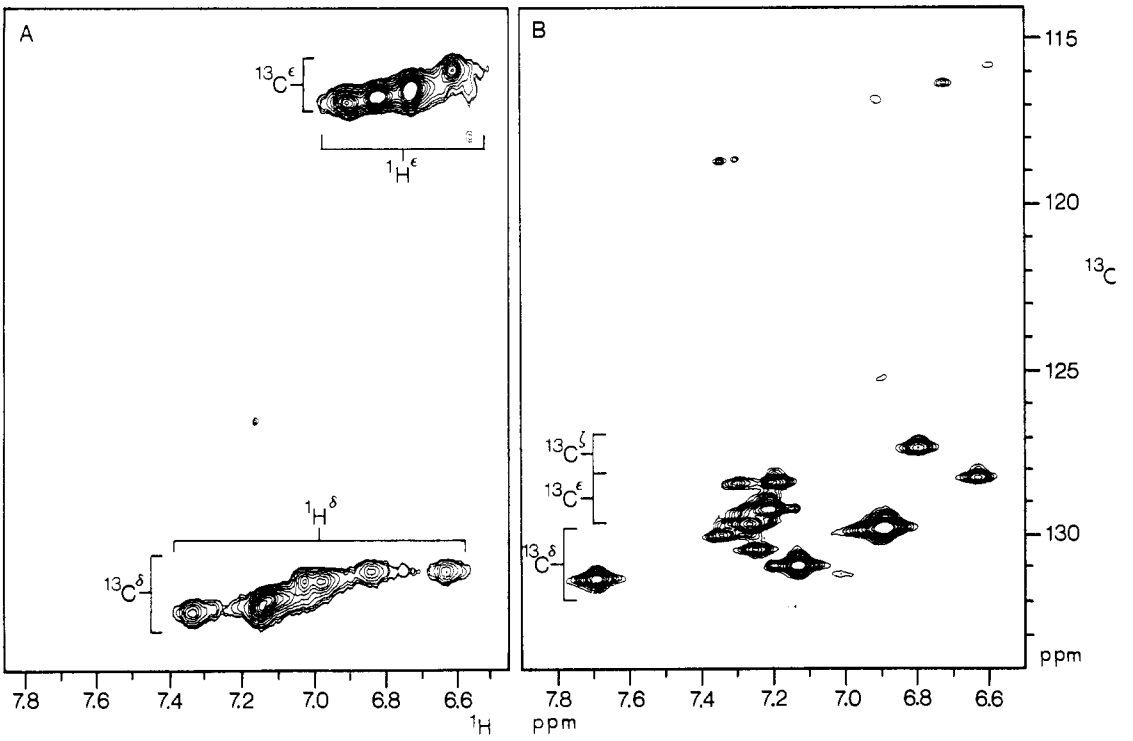

FIGURE 4: Aromatic region of 500-MHz $^1H\{^{13}C\}$SBC spectra of (A) [26% U-^{13}C]Tyr-H124L-TC recorded as 176 blocks with 256 averaged FIDs per t_1 value and (B) [26% U-^{13}C]Phe-H124L-TC in ^2H_2O recorded as 248 blocks with 132 averaged FIDs per t_1 value. Other spectral parameters and data processing procedures were as described above (Figure 2). Regions containing direct cross peaks from Tyr $^1H^{\delta,\epsilon}$–$^{13}C^{\delta,\epsilon}$ and Phe $^1H^{\delta,\epsilon,\zeta}$–$^{13}C^{\delta,\epsilon,\zeta}$ are indicated.

interfering cross peaks from other aromatics in the $^1H\{^{13}C\}$SBC spectrum, the $^1H^{\alpha}$–$^{13}C^{\alpha}$ direct cross peak of Tyr^{54}, whose fingerprint region $^1H^{\alpha}$–$^1H^N$ cross peak was not identified previously (Wang et al., 1990a), was assigned at 4.39,54.7 ppm. NOE relay cross peaks were identified (Figure 3B) that connect $^1H^{\alpha}$–$^{13}C^{\alpha}$ and $^1H^{\beta}$–$^{13}C^{\beta}$ direct cross peaks from Tyr^{27}, Tyr^{85}, and Tyr^{115}; these included an NOE relay cross peak at 3.19,55.2 ppm (Figure 3A), which provided further support for the Tyr^{27} spin system assignment. The Tyr^{91} $^1H^{\alpha}$–$^{13}C^{\alpha}$ direct cross peak was linked to the $^1H^{\beta}$–$^{13}C^{\beta}$ direct cross peak of the same residue through an NOE relay cross peak at 3.40,56.2 ppm. This NOE cross peak overlaps a direct cross peak from Tyr^{113} plus that from another residue. The $^1H^{\beta,\beta'}$–$^{13}C^{\beta}$ direct cross peaks of Tyr^{113} are not shown in Figure 3E; however, their positions are indicated by a pair of NOE relay cross peaks at (2.57,2.97),55.9 ppm in Figure 3A. Although no NOE relay cross peaks were observed for Tyr^{54} and Tyr^{93} in Figure 3A,B, NOE relay cross peaks (Figure 3F,G) from Tyr^{93} $^1H^{\delta,\epsilon}$–$^{13}C^{\alpha,\beta}$ and from Tyr^{54} $^1H^{\epsilon}$–$^{13}C^{\alpha,\beta}$ could be used to link the $^1H^{\alpha}$–$^{13}C^{\alpha}$ and $^1H^{\beta}$–$^{13}C^{\beta}$ direct cross peaks as indicated by the solid lines.

The aliphatic proton AMX spin systems of the His and Trp residues were assigned through comparisons of $^1H\{^{13}C\}$SBC and $^1H\{^{13}C\}$SBC-NOE spectra of [26% U-^{13}C]H124L-TC in ^2H_2O. The $^1H^{\beta}$–$^{13}C^{\beta}$ direct cross peak pairs from His^8, His^{46}, His^{121}, and Trp^{140} in the $^1H\{^{13}C\}$SBC spectrum (Figure 3D) were assigned on the basis of NOE connectivities (Figure 3C) to the $^1H^{\alpha}$–$^{13}C^{\alpha}$ direct cross peaks (Figure 3A) of these residues. The $^1H^{\beta}$–$^{13}C^{\alpha}$ NOE relay cross peaks in the 2.30–3.80,51.0–54.0 ppm region of Figure 3A provided further support for these assignments and extended them to the $^1H^{\beta}$–$^{13}C^{\beta}$ direct cross peaks as is indicated in Figure 3E.

Identification and Assignment of Aromatic Portions of the Spin Systems. The use of selectively labeled samples, [26% U-^{13}C]Tyr-H124L-TC, [26% U-^{13}C]Phe-H124L-TC, or [26% U-^{13}C]His-H124L-TC, facilitated the identification of the spin systems of these residues. The aromatic spin systems of Tyr and Phe were identified by comparing $^1H\{^{13}C\}$SBC and $^1H\{^{13}C\}$SBC-HH data recorded selectively for the aromatic region so as to increase spectral resolution. Figure 4A shows the direct cross peaks of the Tyr rings. The $^1H^{\delta}$–$^{13}C^{\delta}$ cross peaks are centered in the 6.60–7.40,130.0–133.0 ppm region, whereas the $^1H^{\epsilon}$–$^{13}C^{\epsilon}$ cross peaks are located in the 6.50–7.0,115.0–117.0 ppm region. In the $^1H\{^{13}C\}$SBC-NOE spectrum, the Tyr aromatic connectivity pattern forms a rectangle with the $^1H^{\delta}$–$^{13}C^{\delta}$ and $^1H^{\epsilon}$–$^{13}C^{\epsilon}$ direct cross peaks at two diagonally opposite corners and the $^1H^{\delta}$–$^{13}C^{\epsilon}$ and $^1H^{\epsilon}$–$^{13}C^{\delta}$ NOE relayed cross peaks at the two other corners. Seven such rectangular connectivity patterns were observed (solid lines in Figure 5B). The one labeled "Y?" (Figure 5) has chemical shifts of $^1H^{\delta}$ = 7.13 ppm and $^1H^{\epsilon}$ = 6.81 ppm that correspond to those of a cross peak in the HOHAHA (^2H_2O) spectrum (circled peak in Figure 1B).

All the direct cross peaks of the phenylalanines are concentrated in the 6.60–7.80,127.0–132.0 ppm region (Figure 4B). The ^{13}C chemical shifts of the Phe $^1H^{\delta}$–$^{13}C^{\delta}$, $^1H^{\epsilon}$–$^{13}C^{\epsilon}$, and $^1H^{\zeta}$–$^{13}C^{\zeta}$ direct cross peaks are located respectively around 130.4, 129.9, and 128.3 ppm. The aromatic connectivity pattern for Phe forms two rectangles with a single common corner located at the position of the $^1H^{\epsilon}$–$^{13}C^{\epsilon}$ direct cross peak. The corners diagonally opposite this common corner correspond to $^1H^{\delta}$–$^{13}C^{\delta}$ and $^1H^{\zeta}$–$^{13}C^{\zeta}$ direct cross peaks. Four Phe aromatic connectivity patterns were found in Figure 5B as indicated by dashed lines. One of these spin systems, that with $^1H^{\delta}$ = 7.23 ppm, $^1H^{\epsilon}$ = 7.34 ppm, and $^1H^{\zeta}$ = 7.28 ppm, was not observed in the aromatic regions of the DQF-COSY (Figure 1A) or HOHAHA (Figure 1B) spectra.

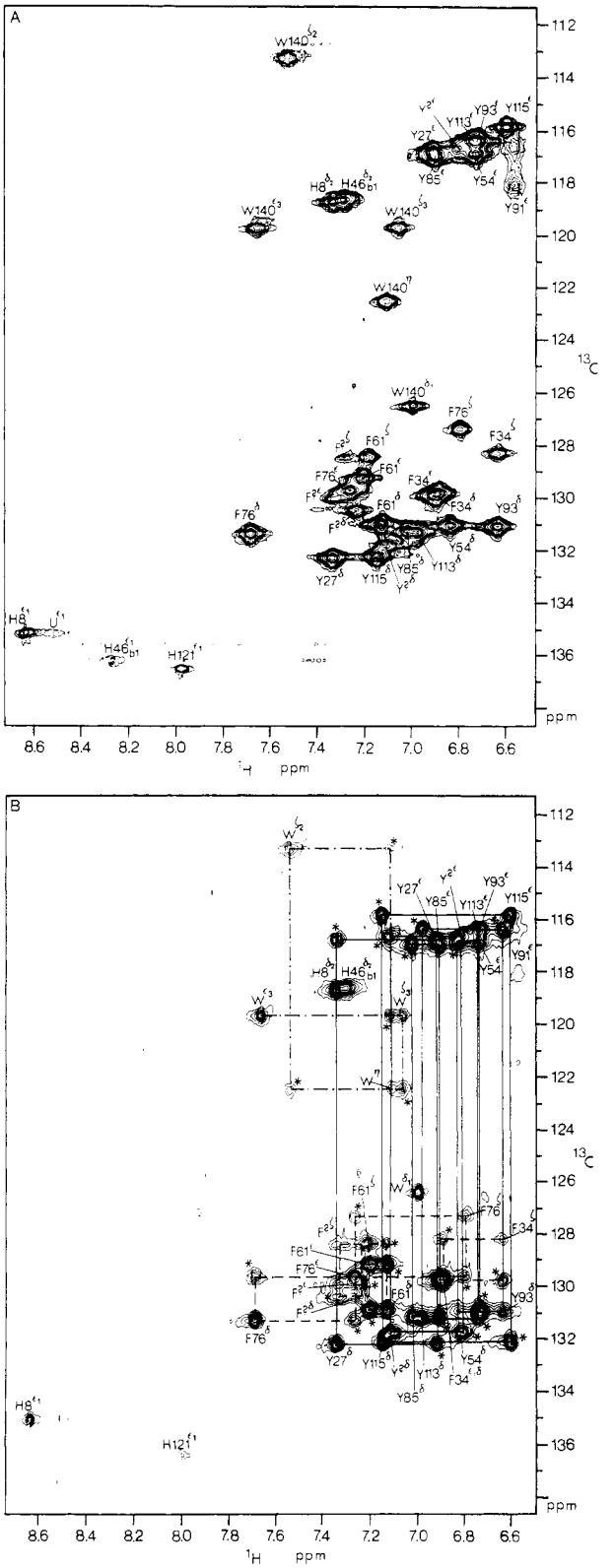

FIGURE 5: Two-dimensional NMR spectra (600 MHz) of [26% U-^{13}C]H124L-TC in ^2H_2O, pH* 5.5. (A) $^1H\{^{13}C\}$SBC spectrum recorded as 512 blocks with 44 averaged FIDs per t_1 value. (B) $^1H\{^{13}C\}$SBC-HH spectrum recroded as 512 blocks with 48 averaged FIDs per t_1 value and a 30-ms spin-lock mixing time. Data processing parameters were identical with those given above. Direct cross peaks are labeled by the one-letter amino acid code and residue number; Hartmann–Hahn relay cross peaks are indicated by asterisks. The letter U stands for histidine of unfolded or degraded protein.

The connectivity pattern for the single Trp was determined by comparing the aromatic regions of the $^1H\{^{13}C\}$SBC (Figure

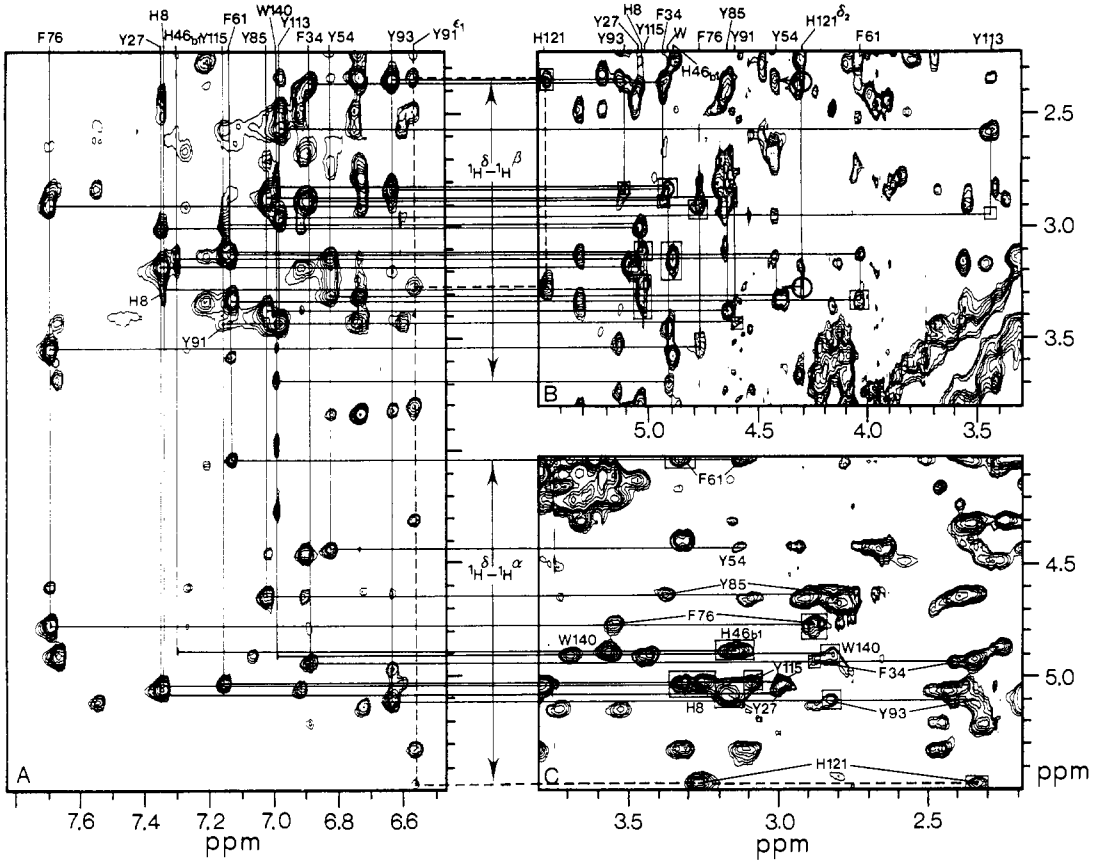

FIGURE 6: Regions of the 500-MHz $^1H\{^1H\}$ phase-sensitive NOESY spectrum of H124L-TC in ^2H_2O solution. 512 data blocks were recorded with 172 averaged FIDs per t_1 value. The NOE mixing time was 200 ms. The solid lines indicate connectivities between aromatic ring δ-proton resonances and the aliphatic $\alpha\beta\beta'$ spin systems of each aromatic residue. (A) Region showing NOE cross peaks between $^1H^{\delta}$ and $^1H^{\alpha,\beta}$ resonances. (B and C) Regions containing NOE connectivities between $^1H^{\alpha}$ and $^1H^{\beta}$. The intraresidue NOEs between $^1H^{\alpha}$ and $^1H^{\beta}$ protons of each aromatic residues are indicated. The positions of the $^1H^{\alpha}$–$^1H^{\beta}$ COSY cross peaks from each aromatic residue are boxed.

5A) and $^1H\{^{13}C\}$SBC-HH (Figure 5B) spectra of [26% U-^{13}C]H124L-TC. The Trp connectivity pattern is indicated by dots and dashes in Figure 5B. We were unable to distinguish the indole δ_1-proton of Trp in the ^1H DQF-COSY (Figure 1A) or HOHAHA (Figure 1B) spectrum. However, the Trp $^1H^{\delta_1}$–$^{13}C^{\delta_1}$ direct cross peak was assigned readily from $^1H\{^{13}C\}$ 2D data (Figure 5).

$^1H\{^{13}C\}$SBC-NOE relay connectivities linking direct cross peaks from the aromatic and aliphatic portions of each amino acid spin system provided the information needed to match up the two parts. Panels C and D of Figure 2 show $^1H^{\delta,\epsilon}$–$^{13}C^{\alpha,\beta}$ NOE relay cross peaks from the three Phe residues that link assigned $^1H^{\alpha}$–$^{13}C^{\alpha}$ or $^1H^{\beta}$–$^{13}C^{\beta}$ direct cross peaks in the aliphatic region to $^1H^{\delta}$–$^{13}C^{\delta}$ or $^1H^{\epsilon}$–$^{13}C^{\epsilon}$ direct cross peaks in the aromatic region. These provided assignments for Phe^{34}, Phe^{61}, and Phe^{76} (Figure 5). A fourth Phe spin system, which has lower intensity than the others, was observed only in the $^1H\{^{13}C\}$SBC spectrum; it has a Hartmann–Hahn connectivity pattern very similar to that of Phe^{61} (Figure 5B) and is denoted by "F?" in Figure 5.

Previously assigned $^1H^{\alpha}$–$^{13}C^{\alpha}$ direct cross peaks (Figure 3A) were linked to $^1H^{\delta,\epsilon}$–$^{13}C^{\alpha}$ NOE relay cross peaks of Tyr^{27}, Tyr^{54}, Tyr^{85}, Tyr^{93}, Tyr^{113}, Tyr^{115}, and Trp^{140} (Figure 3F). Figure 3G shows $^1H^{\delta,\epsilon}$–$^{13}C^{\beta}$ NOE relay cross peaks assigned to the above six tyrosines. An NOE relay cross peak from the seventh tyrosine, Tyr^{91}, was not observed in Figure 3F,G. However, $^1H\{^1H\}$ 2D data provided the missing information.

Figure 6 shows three portions of the $^1H\{^1H\}$ NOESY (^2H_2O) spectrum of [na]H124L-TC. The solid lines indicate connectivities from each aromatic ring ($^1H^{\delta}$) to aliphatic protons ($^1H^{\alpha}$, $^1H^{\beta}$, $^1H^{\beta'}$) of phenylalanines, tyrosines, and tryptophan. All of these connectivities are consistent with those observed in the $^1H\{^{13}C\}$SBC-NOE spectrum (Figure 3). Figure 6A shows a weak NOE cross peak at 7.15,3.40 ppm which is assigned to $^1H^{\delta}$–$^1H^{\beta}$ of Tyr^{91}. Furthermore, the $^1H\{^1H\}$ HOHAHA spectrum (Figure 1B) shows a weak cross peak at 6.58,7.15 ppm that overlaps with the Tyr^{115} cross peak. This weak cross peak was assigned to $^1H^{\epsilon}$–$^1H^{\delta}$ of Tyr^{91}.

The imidazole spin systems of the His residues were identified on the basis of $^1H\{^1H\}$ DQF-COSY (Figure 1A), HOHAHA (Figure 1B), and $^1H\{^{13}C\}$SBC (Figure 5) data. $^1H\{^1H\}$ NOESY data (Figure 6) established clear NOE connectivities between one ring proton ($^1H^{\delta_2}$) and aliphatic protons ($^1H^{\alpha}$, $^1H^{\beta}$, $^1H^{\beta'}$) of His^8 and His^{46}. Similar cross peaks for His^{121} were not observed in the aromatic region. The reason is that the His^{121} $^1H^{\delta_2}$ resonance is located upfield of water in the aliphatic region. The $^1H\{^{13}C\}$SBC spectrum of [26% U-^{13}C]His-H124L-TC (Figure 7B) shows one direct cross peak at 4.32,117.8 ppm which is assigned to $^1H^{\delta_2}$–$^{13}C^{\delta_2}$ of His^{121}. This assignment comes from $^1H\{^{13}C\}$MBC data (Figure 7C,D) that show cross peaks at 4.32,130.8 and 4.32,136.4 ppm assigned to $^1H^{\delta_2}$–$^{13}C^{\gamma,\epsilon_1}$ (two and three bond) connectivities. The two circled NOE cross peaks at 4.32 ppm, which link the $^1H^{\delta_2}$ to the $^1H^{\beta_1,\beta_2}$ of His^{121} (Figure 6B), confirm the above assignments. These connectivities, as well as similar ones for His^8, are seen more clearly in the $^1H\{^{13}C\}$MBC spectrum (Figure 7C,D) of the selectively labeled complex, [U-^{13}C]-His-H124L-TC. Inexplicably, the $^1H^{\epsilon_1}$–$^{13}C^{\delta_2}$ and $^1H^{\epsilon_1}$–$^{13}C^{\gamma}$ multiple-bond cross peaks were not observed for His^{46}.

Assignment of Nonprotonated Carbons. The quaternary

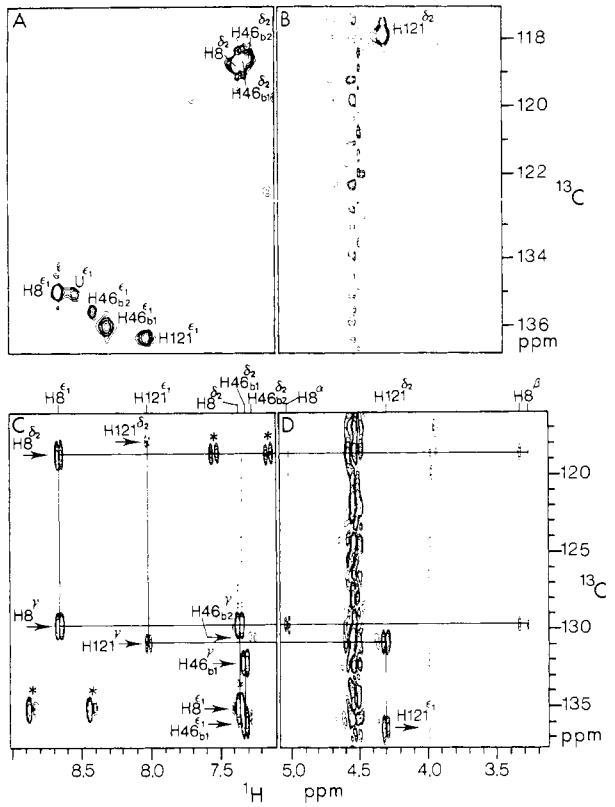

FIGURE 7: Heteronuclear two-dimensional NMR spectra of [26% U-^{13}C]His-H124L-TC in ^2H_2O, which provided unambiguous assignments of the His ^{1}H and ^{13}C spin systems. (A) 600-MHz ^{1}H-{^{13}C}SBC spectrum obtained as 182 data blocks with 248 averaged FIDs per t_1 value. Direct cross peaks are labeled by the one-letter amino acid code, residue number, and atom type. (B) 500-MHz ^{1}H{^{13}C}MBC spectrum obtained as 190 blocks with 256 averaged FIDs per t_1 value. Multiple-bond cross peaks are labeled by the one-letter amino acid code, residue number, and atom type. Nonsuppressed, undecoupled single-bond correlation cross peaks of His^8, $^1H^{\epsilon_1}$–$^{13}C^{\epsilon_1}$, and $^1H^{\delta_2}$–$^{13}C^{\delta_2}$ are indicated by asterisks. The letter U stands for histidine or unfolded or degraded protein. Data processing was as described above.

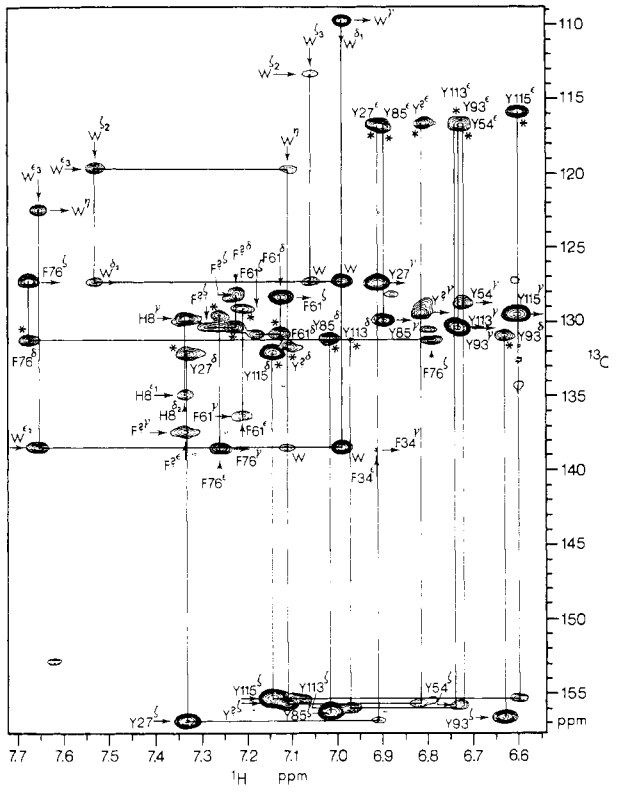

FIGURE 8: 500-MHz two-dimensional ^{1}H{^{13}C}MBC spectrum of [26% U-^{13}C]H124L-TC recorded selectively for the aromatic resonances. The delay time for suppressing one-bond correlations was 2.78 ms, and the delay time for optimizing two- and three-bond correlations was 70 ms. 372 increments were acquired with 160 averaged FIDs per t_1 value. The spectrum is presented in the mixed mode. Cross peaks are labeled by one-letter amino acid code, residue number [except for peaks from Trp^{140} (labeled W) and the extra, unassigned, Phe (F$^?$) and Tyr (Y$^?$) spin systems], and atom type. Three-bond correlation cross peaks, $^1H^{\epsilon_3,\epsilon_5}$–$^{13}C^{\epsilon_3,\epsilon_3}$ and $^1H^{\delta_2,\delta_6}$–$^{13}C^{\delta_6,\delta_2}$, of tyrosines and phenylalanines are indicated by asterisks.

carbons of the aromatic residues ($^{13}C^{\gamma}$ from each residue, $^{13}C^{\zeta}$ from Tyr, $^{13}C^{\delta_2}$ and $^{13}C^{\epsilon_2}$ from Trp) were identified on the basis of two- and three-bond correlations observed in ^{1}H{^{13}C}MBC spectra. Tyrosine $^{13}C^{\gamma}$ resonances (centered around 129.5 ppm) and Tyr $^{13}C^{\zeta}$ resonances (centered around 155.5 ppm) occur in isolated regions. For Tyr, all expected two- and three-bond correlations to $^{13}C^{\zeta}$ ($^1H^{\delta,\epsilon}$–$^{13}C^{\zeta}$) were resolved, but only the three-bond correlations to $^{13}C^{\gamma}$ ($^1H^{\epsilon}$–$^{13}C^{\gamma}$) were observed (Figure 8). Assignments were obtained for the side-chain quaternary carbons of Tyr^{27}, Tyr^{54}, Tyr^{85}, Tyr^{93}, Tyr^{113}, Tyr^{115}, and Tyr$^?$ (Figure 8, Table I). The Phe $^{13}C^{\gamma}$ resonances, which also fall in an isolated spectral region, were matched by virtue of $^1H^{\epsilon}$–$^{13}C^{\gamma}$ (three-bond correlation) cross peaks to the assigned $^1H^{\epsilon}$ resonances of Phe^{34}, Phe^{61}, Phe^{76}, and Phe$^?$ (Figure 8, Table I).

The $^{13}C^{\gamma}$ of Trp was assigned from the $^1H^{\delta_1}$–$^{13}C^{\gamma}$ cross peak located at the extreme high-field side of the aromatic ^{13}C region (Figure 8). The ^{13}C resonance that showed three-bond coupling with indole protons $^1H^{\delta_1}$, $^1H^{\zeta_2}$, and $^1H^{\zeta_3}$ was assigned to Trp^{140} $^{13}C^{\delta_2}$; the ^{13}C resonance that showed three-bond coupling with indole protons $^1H^{\delta_1}$, $^1H^{\epsilon_3}$, and $^1H^{\eta}$ was assigned to Trp^{140} $^{13}C^{\epsilon_2}$ (Figure 8).

The His $^{13}C^{\gamma}$ resonances are located in a relatively crowded region. A $^1H^{\delta_2}$–$^{13}C^{\gamma}$ two-bond correlation cross peak in the spectrum of the uniformly ^{13}C-labeled complex (Figure 8) identified the quaternary carbon of His^8, but selective labeling

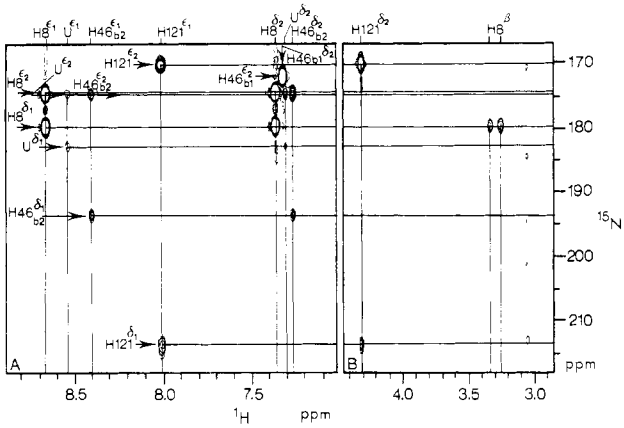

FIGURE 9: Two regions (A and B) of the 600-MHz ^{1}H{^{15}N}MBC spectrum of [95% U-^{15}N]H124L-TC in ^2H_2O. Data were recorded selectively for the His region in the ^{15}N dimension. 212 blocks were collected with 256 averaged FIDs per t_1 value. The delay time for suppressing single-bond correlations was 5.56 ms. Assigned cross peaks in both spectra are labeled with the one-letter amino acid code, residue number, and atom type. The letter U stands for histidine of unfolded or degraded protein.

was required in order to identify the analogous quaternary carbon signals from His^{46} and His^{121} (Figure 7B).

Assignment of Resonances from Histidine Imidazole Nitrogens. The imidazole nitrogen assignments were deduced from ^{1}H{^{15}N}MBC data, which were acquired with [95%

U-^{15}N]H124L-TC in ^2H_2O, as extensions of the imidazole $^1H^{\delta_2}$ and $^1H^{\epsilon_1}$ assignments reported above. The His imidazole $^1H^{\delta_2}$–$^{15}N^{\delta_1,\epsilon_2}$, $^1H^{\epsilon_1}$–$^{15}N^{\delta_1,\epsilon_2}$, and $^1H^{\beta}$–$^{15}N^{\delta_1}$ multiple-bond connectivity patterns, shown by solid lines in Figure 9, provided assignments of the $^{15}N^{\delta_1}$ and $^{15}N^{\epsilon_2}$ of His[8] and His[46] in the b2 conformational substate (see below). The His[121] $^{15}N^{\delta_1}$ and $^{15}N^{\epsilon_2}$ show intraresidue two-bond correlations to $^1H^{\epsilon_1}$ (Figure 9A) and three- or two-bond correlations, respectively, to $^1H^{\delta_2}$ (Figure 9B). It is unclear why His[46] in the b1 conformational substate gave rise to only one resolved multiple-bond ^1H–^{15}N cross peak: that from the $^1H^{\delta_2}$–$^{15}N^{\epsilon_2}$ (two bond) correlation (Figure 9C). A $^1H\{^{15}N\}$MBC spectrum of [95% U-^{15}N]-His-H124L-TC in ^2H_2O confirmed these results (data not shown).

Discussion

Detection and Characterization of Conformational Substates. Previous studies of conformational heterogeneity in staphylococcal nuclease have relied exclusively on observations of the His imidazole ^1H resonances (Markley et al., 1970; Fox et al., 1986, Evans et al., 1987, 1989; Alexandrescu et al., 1988, 1899; Alexandrescu & Markley, 1989; Wilde et al., 1988). The present results demonstrate that conformational substates also can be detected through ^{13}C or ^{15}N resonance heterogeneity.

A variety of unligated and ligated states of staphylococcal nuclease have been detected by physical techniques. It is useful to consider these in terms of "macroscopic states" and "conformational substates". A macroscopic state is defined as a form having a particular protein–ligand molecular composition and global fold (folded or unfolded). Examples include (1) the unligated nuclease monomer (NM) and dimer (ND), (2) the binary nuclease·Ca^{2+} complex (BC),[3] (3) the binary nuclease·pdTp complex (BN), (4) the ternary nuclease·pdTp·Ca^{2+} complex (TC), and (5) unfolded nuclease (U). Conformational heterogeneity detected within these macroscopic states is denoted here by a subscript.[4] Two kinds of conformational heterogeneity have been characterized so far in the native nuclease monomer:

(1) A conformational equilibrium between two substates (a1 and a2) is linked to pdTp binding. Both the NM_{a1} and NM_{a2} forms bind Ca^{2+} and pdTp, but the association constant is higher for the a1 form so that the TC_{a1} species predominates over the TC_{a2} species (Alexandrescu et al., 1989). Magnetization-transfer experiments (Evans et al., 1987, 1989) have demonstrated single-step equilibria linking each substate of the unligated folded protein and one substate of the unfolded protein. Thus NM_{a1} is linked to U_{a1} and NM_{a2} is linked to U_{a2}. The (a1 = a2) conformational equilibrium leads to doubling of the $^1H^{\epsilon_1}$ resonances of His[8], His[121], and His[124] (Evans et al., 1987, 1989; Alexandrescu et al., 1989) as well as many other resonances throughout the protein molecule (Alexandrescu, 1989; J. Wang, S. N. Loh, and J. L. Markley, unpublished results).

(2) A conformational equilibrium between two other substates (b1 and b2) is not perturbed by complexation with Ca^{2+} or pdTp. This heterogeneity persists in the BC and TC forms. Thus far the (b1 = b2) equilibrium has been observed only as a doubling of the His spin system (^1H, ^{13}C, and ^{15}N resonances) of His[46] (see below).

Since two conformational equilibria (a1 = a2 and b1 = b2) are present, the protein actually exists as a mixture of four states: a1b1, a1b2, a2b1, and a2b2. Present results have not provided a way to distinguish the mixed states. The spin system of His[46] does not discriminate between states a1b1 and a2b1 or between states a1b2 and a2b2, and those spin systems that are responsive to the a1 = a2 equilibrium do not discriminate between states a1b1 and a1b2 or between states a2b1 and a2b2. This suggests that the structural consequences of the two equilibria are localized and to some extent nonoverlapping. Resonances affected by both transitions, should they be found, should map onto the boundary between the two regions of structural change.

Comparison with Previous Assignments. The assignments of the $^1H^{\epsilon_1}$ and $^1H^{\delta_2}$ resonances of His[8] and His[46] (b1 and b2) and the $^1H^{\epsilon_1}$ resonance of His[121] determined here by the sequential NMR assignment method are all consistent with those deduced previously for nuclease wt on the basis of mutagenesis (Alexandrescu et al., 1988; Alexandrescu, 1989). The results reported here are in general agreement with the less extensive aromatic residue assignments of Torchia et al. (1989), who identified resonances from only one conformational state of nuclease wt TC at pH 7.4.

Our assignment of the $^1H^{\delta_2}$ resonance of His[121] differs from that reported previously for the unligated (NM) and ternary complex (TC) forms of nuclease wt (Stanczyk et al., 1988). The assignment strategy used by these authors was to deuterate the aromatic ring protons of Tyr, Trp, and Phe but not those of His. Their deuteration procedure did not extend to the aliphatic region where our results show the $^1H^{\delta_2}$ resonance of His[121] to be located (4.3 ppm). We have shown that the difference in chemical shift is not explained by the H124L mutation (Hinck et al., 1990). Thus it appears that Stanczyk et al. (1988) misassigned two small resonances around 6.9 ppm in nuclease wt and nuclease wt TC to His[121] $^1H^{\delta_2}$. These peaks probably correspond instead (Table I) to residual protonated aromatic residues (e.g., Tyr[54], Tyr[113], or Phe[34]). Since the heterogeneity of the peaks around 6.9 ppm was not removed on formation of the ternary complex, the authors claimed that this provided evidence for the existence of a new type of structural heterogeneity in nuclease. We have found, however, that both the $^1H^{\epsilon_1}$ and $^1H^{\delta_2}$ resonances of His[121] report the a1 = a2 conformational equilibrium in nuclease wt and in mutants (Hinck et al., 1990). Thus, as with His[8] and His[124] (Alexandrescu, 1989), single signals are observed for the His[121] spin systems (^1H, ^{13}C, or ^{15}N) in the ternary complex. A number of single-site mutations have been found to shift the equilibrium between the a1 and a2 forms in unligated nuclease (Alexandrescu et al., 1989; Alexandrescu, 1989; Alexandrescu & Markley, 1989). Such mutations were found to alter the a1/a2 ratios of both the $^1H^{\epsilon_1}$ and $^1H^{\delta_2}$ resonances of His[121] in a coordinate fashion (Hinck et al., 1990).

The present results reveal a dual spin system for His[46], which defines conformational substates b1 and b2. The doubled proton peaks are assigned unambiguously to His, since they appear in $^1H\{^{13}C\}$ spectra of nuclease samples labeled selectively with [^{13}C]His (Figure 7; Alexandrescu, 1989) and in a $^1H\{^{15}N\}$ spectrum of a nuclease sample labeled selectively with [^{15}N]His (data not shown). Sequence-specific assignment of the two peaks to His[46] is supported by the fact that both peaks are missing in the spectrum of a mutant (H46Y-TC) that lacks His[46] (Alexandrescu, 1989). The b1/b2 heterogeneity is visible in $^1H\{^{13}C\}$SBC (Figure 7A), $^1H\{^{13}C\}$MBC (Figure 7C), and $^1H\{^{15}N\}$MBC (Figure 9A,B) spectra. Dif-

[4] The following definitions equate previous nomenclature used in this laboratory (Alexandrescu et al., 1988, 1989) with the nomenclature introduced here for conformational substrates (old designation = new designation): N = NM_{a1}; N′ = NM_{a2}; N″ = ND; U = U_{a1}; U* = U_{a2}. The new nomenclature is needed in order to describe the increased complexity of conformational heterogeneity identified here.

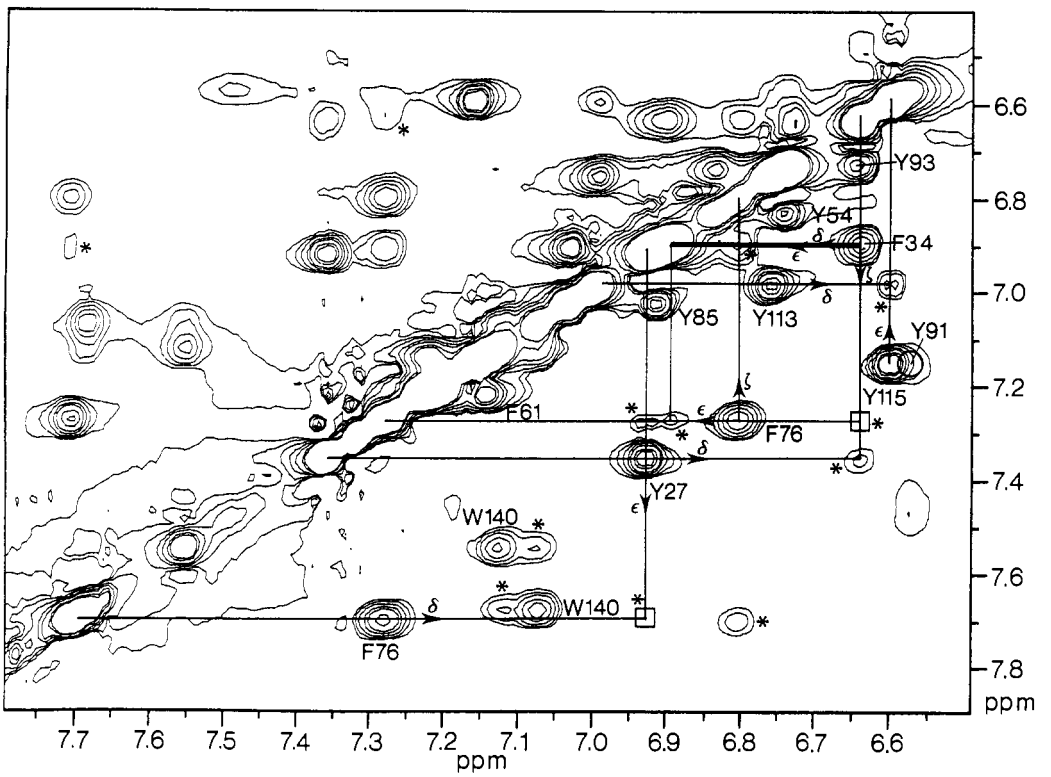

FIGURE 10: Aromatic region of the 500-MHz $^1H\{^1H\}$ phase-sensitive NOESY spectrum obtained with H124L-TC in ^2H_2O solution. The figure does not include the His region of the spectrum. The spectrum was acquired as 512 blocks with a mixing time of 150 ms and 132 averaged FIDs per t_1 value. NOE cross peaks are denoted by asterisks. Intraresidue NOE cross peaks are labeled by the one-letter amino acid code and residue number. Interresidue NOE connectivities of aromatic ring protons are indicated by solid lines. The empty rectangular boxes indicate the positions of NOESY cross peaks observed in the left part of this spectrum (denoted by asterisks) and in a spectrum recorded with a longer NOE mixing time (200 ms).

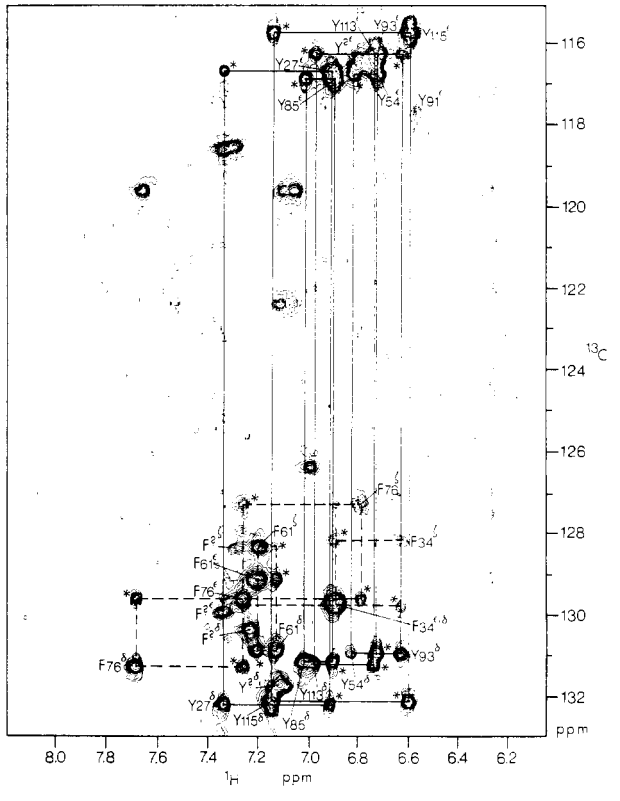

FIGURE 11: 500-MHz $^1H\{^{13}C\}$SBC-NOE spectrum of [26% U-^{13}C]H124L-TC in ^2H_2O recorded selectively for the aromatic region as 244 increments with 184 averaged FIDs per t_1 value. The mixing time used for the NOE buildup was 250 ms. Spin system connectivities of tyrosines and phenylalanines are represented respectively by solid or dashed lines. The NOE relay cross peaks are indicated by the one-letter amino acid code and residue number.

ferences in the environment of the His[46] side chain in the b1 and b2 states affect ^{13}C and ^{15}N chemical shifts as well as ^1H chemical shifts (Table I). In unligated nuclease wt or H124L, the His[46] $^1H^{\epsilon 1}$ signal appears as a broad singlet at 318 K, but separate signals from the b1 and b2 states shift apart at lower temperature (S. N. Loh, unpublished data). Doubled His[46] $^1H^{\epsilon 1}$ peaks are observed in the BC and TC states, but the b1/b2 ratio appears to be unaffected by ligand binding. Doubled His[46] $^1H^{\epsilon 1}$ peaks also have been observed in spectra of mutant nucleases (A. P. Hinck and S. N. Loh, unpublished data). The lifetimes of the b1 and b2 states are on the order of 25–1000 ms, since magnetization transfer between the two separate His[46] $^1H^{\epsilon 1}$ peaks has been demonstrated (Alexandrescu, 1989; S. N. Loh, unpublished results).

The data reported here for the ternary complex (H124L-TC) show the presence of extra spin systems for one His (His[U] or U), one Phe (Phe[?]), and one Tyr (Tyr[?]) (Figures 1, 5, and 11). The origin of these peaks is under continued investigation. The histidine spin system resembles that of unfolded nuclease (Alexandrescu, 1989), and no intraresidue NOEs were observed for the ring protons assigned to Phe[?] or Tyr[?] (Figures 11 and 10). The resonances may arise from denatured or degraded protein.

Comparison of the Solution and Solid-State Structures. The $^1H\{^1H\}$ NOESY (^2H_2O) data provide NOE connectivities (dashed lines in Figure 6) that locate the His[121] ring adjacent to the Tyr[91] ring. They link the α- (5.47 ppm), β- (2.35 ppm), β'- (3.28 ppm), and δ_2-protons (4.3 ppm) of His[121] and an ϵ-proton (6.58 ppm) of Tyr[91]. This result is in agreement with the X-ray structures of the nuclease wt ternary complex, which place the His[121] δ_2-hydrogen adjacent to the middle of the Tyr[91] ring. Ring-current shift calculations from either the Cotton et al. (1979) or Loll and Lattman (1989) X-ray coordinates

predict an upfield shift of about 3.2 ppm for the His^{121} $^1H^{\delta_2}$ from the anisotropy of the Tyr^{91} ring. The ring-current effect fully explains the unusual chemical shift observed for this proton. The large (0.93 ppm) chemical shift difference between the two His^{121} β-protons results from one of the His^{121} β-protons (the *pro-S* $^1H^{\beta}$) experiencing a larger ring-current shift than the other (the *pro-R* $^1H^{\beta}$).

Evidence for slow (on the NMR time scale) flipping of the Tyr^{91} ring is provided by separate resonances for hydrogens and carbons on either side of the ring. Two peaks observed in the $^1H\{^{13}C\}$SBC spectrum at (116.6,118.1),6.58 ppm (Figure 5A) are assigned to $^1H^{\epsilon}$–$^{13}C^{\epsilon}$ direct cross peaks of Tyr^{91}. Weak cross peaks observed at 6.58,(7,15,7.46) ppm in $^1H\{^1H\}$ HOHAHA (Figure 1B) and NOESY (Figure 10) spectra are assigned to $^1H^{\epsilon}$–($^1H^{\delta_1}$,$^1H^{\delta_2}$) of Tyr^{91}. Our failure to observe the $^1H^{\delta_1,\delta_2}$–$^{13}C^{\delta_1,\delta_2}$ $^1H\{^{13}C\}$SBC direct cross peaks may have been a consequence of exchange broadening. Rotation of the Tyr^{91} ring may be hindered by the steric proximity of the His^{121} $^1H^{\delta_2}$. Similar slow ring flipping of the Tyr^{91} ring protons of nuclease wt TC was described by Torchia et al. (1989).

Interresidue NOE cross peaks observed in the aromatic region of the NOESY spectrum (Figure 10) indicate the presence of short contact distances ($d < 5$ Å) between pairs of ring protons of several aromatic amino acids. NOESY data sets were collected at three different mixing times (100, 150, and 200 ms). A number of these distances were evaluated quantitatively by fitting the initial buildup rate of NOEs according to a procedure described by Fejzo et al. (1989). These distances are compared (Table II) with the corresponding distances derived from the two available X-ray structures of the nuclease wt·pdTp·Ca^{2+} ternary complex. The NMR distances agree within experimental error with those from the more refined structure (Loll & Lattman, 1989) but not with several distances from the less refined structure (Cotton et al., 1979).

ACKNOWLEDGMENTS

We thank Professor Julius Adler for providing auxotrophic *E. coli* strains, Denise Benway for isolating the ^{13}C-labeled amino acids used in this study, Dr. M. Kainosho for providing a sample of ^{15}N-labeled His, Dr. Christopher L. Kojiro for providing the original ring current calculations, Andrzej M. Krezel for calculating interproton distances and upgrading the ring current calculation program, Jasna Fejzo for assisting with the distance measurements, Drs. Loll and Lattman for providing coordinates of their refined X-ray structure of the nuclease wt ternary complex, and Dr. Dennis A. Torchia for sending copies of his manuscripts prior to publication.

REFERENCES

Alexandrescu, A. T. (1989) Ph.D. Thesis, University of Wisconsin—Madison.

Alexandrescu, A. T., & Markley, J. L. (1990) *Biochemistry* (in press).

Alexandrescu, A. T., Mills, D. A., Ulrich, E. L., Chinami, M., & Markley, J. L. (1988) *Biochemistry 27*, 2158–2165.

Alexandrescu, A. T., Ulrich, E. L., & Markley, J. L. (1989) *Biochemistry 28*, 204–211.

Chinami, M., & Shingu, M. (1989) *Arch. Biochem. Biophys. 270*, 126–136.

Cohen, J. S., Feil, M., & Chaiken, I. M. (1971) *Biochim. Biophys. Acta 236*, 468–478.

Cotton, F. A., Hazen, E. E., Jr., & Legg, M. J. (1979) *Proc. Natl. Acad. Sci. U.S.A. 76*, 2551–2555.

Cusumano, C. L., Taniuchi, H., & Anfinsen, C. B. (1968) *J. Biol. Chem. 243*, 4769–4774.

Evans, P. A., Dobson, C. M., Kautz, R. A., Hatfull, G., & Fox, R. O. (1987) *Nature 329*, 266–268.

Evans, P. A., Kautz, R. A., Fox, R. O., & Dobson, C. M. (1989) *Biochemistry 28*, 362–370.

Fejzo, J., Zolnai, Z., Macura, S., & Markley, J. L. (1989) *J. Magn. Reson.* (in press).

Fox, R. O., Evans, P. A., & Dobson, C. M. (1986) *Nature 320*, 192–194.

Grissom, C. B., & Markley, J. L. (1989) *Biochemistry 28*, 2116–2124.

Hinck, A. P., Loh, S. N., Wang, J., & Markley, J. L. (1990) *Biophys. J. 57*, 45a.

Jardetzky, O., Markley, J. L., Thielmann, H., Arata, Y., & Williams, M. N. (1972) *Cold Spring Harbor Symp. Quant. Biol. 36*, 257–261.

Johnson, C. E., & Bovey, F. A. (1958) *J. Chem. Phys. 29*, 1012–1014.

Loll, P. J., & Lattman, E. E. (1989) *Proteins: Struct., Funct., Genet. 5*, 183–201.

Markley, J. L. (1989) *Methods Enzymol. 176*, 12–63.

Markley, J. L., & Jardetzky, O. (1970) *J. Mol. Biol. 50*, 223–233.

Markley, J. L., Putter, L., & Jardetzky, O. (1968) *Science 161*, 1249–1251.

Markley, J. L., Williams, M. N., & Jardetzky, O. (1970) *Proc. Natl. Acad. Sci. U.S.A. 65*, 645–651.

Meadows, D. H., Markley, J. L., Cohen, J. S., & Jardetzky, O. (1967) *Proc. Natl. Acad. Sci. U.S.A. 58*, 1307–1313.

Perkins, S. J. (1982) *Biol. Magn. Reson. 4*, 193–337.

Stanczyk, S. M., Bolton, P. H., Dell'Acqua, M., Pourmotabbed, T., & Gerlt, J. A. (1988) *J. Am. Chem. Soc. 110*, 7908–7910.

Taniuchi, H., Anfinsen, C. B., & Sodja, A. (1967) *J. Biol. Chem. 242*, 4752–4758.

Torchia, D. A., Sparks, S. W., & Bax, A. (1989a) *Biochemistry 28*, 5509–5524.

Torchia, D. A., Sparks, S. W., Young, P. E., & Bax, A. (1989b) *J. Am. Chem. Soc. 111*, 8315–8317.

Tucker, P. W., Hazen, E. E., Jr., & Cotton, F. A. (1979) *Mol. Cell. Biochem. 23*, 3–16.

Wang, J., LeMaster, D. M., & Markley, J. L. (1990a) *Biochemistry 29*, 88–101.

Wang, J., Hinck, A. P., Loh, S. N., & Markley, J. L. (1990b) *Biochemistry 29*, 102–113.

Wilde, J. A., Bolton, P. H., Dell'Acqua, M., Hibler, B. W., Pourmotabbed, T., & Gerlt, J. A. (1988) *Biochemistry 27*, 4127–4132.